

General Disclaimer

One or more of the Following Statements may affect this Document

- This document has been reproduced from the best copy furnished by the organizational source. It is being released in the interest of making available as much information as possible.
- This document may contain data, which exceeds the sheet parameters. It was furnished in this condition by the organizational source and is the best copy available.
- This document may contain tone-on-tone or color graphs, charts and/or pictures, which have been reproduced in black and white.
- This document is paginated as submitted by the original source.
- Portions of this document are not fully legible due to the historical nature of some of the material. However, it is the best reproduction available from the original submission.

A MESO-CLIMATOLOGY STUDY OF THE HIGH-RESOLUTION TOWER NETWORK OVER THE FLORIDA SPACEPORT

Jonathan L. Case* and William H. Bauman III
ENSCO, Inc., Cocoa Beach, FL

1. INTRODUCTION

Forecasters at the US Air Force 45th Weather Squadron (45 WS) use wind and temperature data from the tower network over the Kennedy Space Center (KSC) and Cape Canaveral Air Force Station (CCAFS) to evaluate Launch Commit Criteria and to issue and verify temperature and wind advisories, watches, and warnings for ground operations. The Spaceflight Meteorology Group at the Johnson Space Center in Houston, TX also uses these data when issuing forecasts for shuttle landings at the KSC Shuttle Landing Facility. Systematic biases in these parameters at any of the towers could adversely affect an analysis, forecast, or verification for all of these operations. In addition, substantial geographical variations in temperature and wind speed can occur under specific wind directions. Therefore, the Applied Meteorology Unit (AMU), operated by ENSCO Inc., was tasked to develop a monthly and hourly climatology of temperatures and winds from the tower network, and identify the geographical variation, tower biases, and the magnitude of those biases.

This paper presents a sub-set of results from a nine-year climatology of the KSC/CCAFS tower network, highlighting the geographical variations based on location, month, times of day, and specific wind direction regime. Section 2 provides a description of the tower mesonetwork and instrumentation characteristics. Section 3 presents the methodology used to construct the tower climatology including QC methods and data processing. The results of the tower climatology are presented in Section 4 and Section 5 summarizes the paper.

2. TOWER DATA DESCRIPTION

2.1 Brief History

In 1961 and 1962, a research project called the Ocean Breeze and Dry Gulch Diffusion program was conducted at Cape Canaveral, FL and Vandenberg Air Force Base, CA, respectively, by the Air Force Cambridge Research Laboratories (Haugen and Fuquay 1963; Haugen and Taylor 1963). The program was designed to address air pollution hazards associated with planned launches of the Titan II missile at both ranges. Another goal of the program was to provide Range Safety personnel and staff meteorologists with an operationally useful system for

observing the state of the atmospheric boundary layer. Such a system was required for staff meteorologists to interpret the fine-scale meteorological conditions during launch operations for evaluating safety considerations, pad conditions of winds and wind gusts, and to generate precise short-range forecasts at the launch pads.

As a result of the program, the Weather Information Network Display System (WINDS) was developed and implemented at Cape Canaveral, FL consisting of eight towers in the original operational system in 1964. WINDS was expanded in 1966 and 1984, reaching a total of 29 towers covering an area of 790 km². WINDS was again expanded to 49 towers in 1987 to cover an area of approximately 1600 km² (Harms et al. 2001), and to accommodate forecasting techniques recommended by Watson et al. (1989). The network was then reduced in the early 1990s to its current number of 44 towers.

2.2 Current Mesonetwork

The current tower network consists of 44 towers that measure temperature, humidity, and winds at various locations and heights. According to Figure 1 (CSR 2000), the nearest-neighbor spacing between towers generally ranges from 3 to 6 km, with the smallest spacing over KSC and CCAFS (Figure 2). Station spacing increases markedly over mainland Florida west of KSC/CCAFS. The average tower spacing for the whole network is 5 km.

The towers are grouped into three categories based on their primary use (CSR 2000):

- **Launch critical towers.** These towers are used in the direct evaluation of launch constraints, have the greatest vertical measurement extent, and have dual sensors on opposite sides of the towers.
- **Safety critical towers.** These towers are located at or near areas where propellants and other hazardous chemicals are stored or handled, supporting emergency response activities.
- **Forecast critical towers.** These towers surround the KSC/CCAFS area and support the 45 WS in routine weather forecast and warning operations.

Due to poor data availability in the archive, or measurement heights inconsistent with the majority of the towers in the network, several towers were excluded from the climatology. Figure 2 shows only the tower locations used for the climatology. It is important to note

*Corresponding author address: Jonathan Case, ENSCO, Inc., 1980 N. Atlantic Ave., Suite 230, Cocoa Beach, FL 32931. Email: case.jonathan@ensco.com

that several of the forecast critical towers over mainland Florida suffered from poor data availability due to communication limitations and software deficiencies.

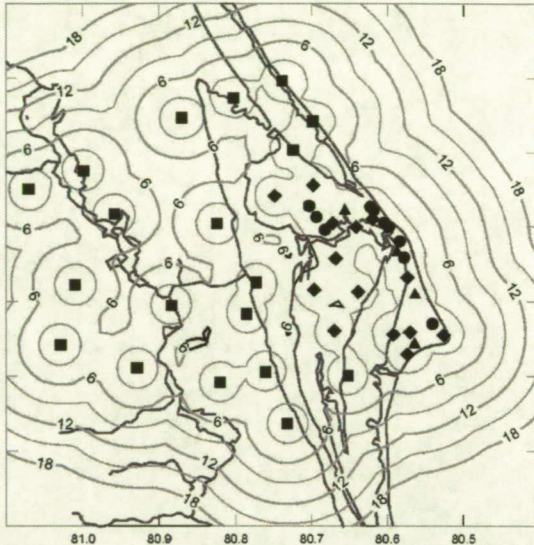


Figure 1. Distance to the nearest tower, in km.

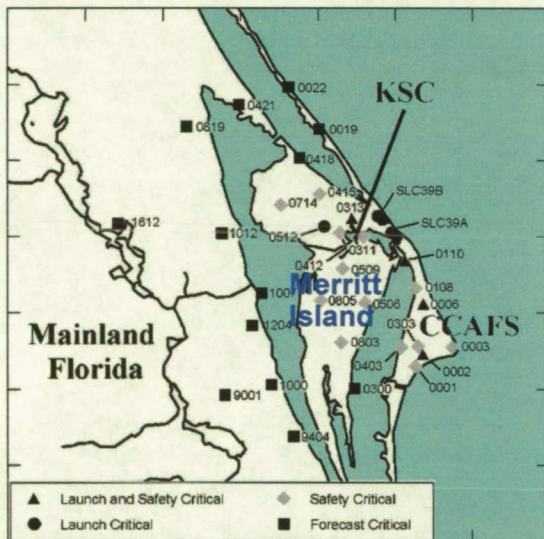


Figure 2. Locations of the towers used in the nine-year climatology. Note that this plot does not represent all towers within the network.

The primary difference between the instrument packages is that the launch/safety critical towers have mechanically aspirated temperature sensors whereas the forecast critical towers have naturally aspirated sensors with a radiation shield. Examples of mechanically and naturally aspirated temperature sensors are shown in Figures 3 and 4, respectively.

Table 1 provides a summary of the heights and variables measured at each tower location. Forecast towers have the simplest sensor suite, consisting of 1.8 m temperature and humidity measurements, and 16.5 m wind readings. Safety towers measure

temperature at 1.8 m and 16.5 m, winds at 3.6 m and 16.5 m, and do not provide any humidity measurements. The launch critical towers measure temperature and winds at multiple heights and on opposite sides of the towers.



Figure 3. A mechanically aspirated 1.8 m temperature sensor at tower ID#0403.



Figure 4. A naturally aspirated 1.8 m temperature sensor with radiation shield at tower ID#1007.

The tallest launch critical tower, 0313 (in KSC), has wind, temperature, and humidity sensors at multiple levels up to 150 m on the southwest (ID#3131) and northeast sides (ID#3132). Launch critical towers 0002, 0006, and 0110 have sensors up to 62 m on the northwest and southeast sides (IDs given in Table 1). The only other launch critical towers used in the climatology are those at space shuttle launch complexes (SLC) 39A and SLC 39B (tower IDs 0394 and 0398), which measure temperatures at 1.8 m and 18.3 m, and winds and humidity at 18.3 m. In order to simplify the climatology, the 18.3 m temperatures and winds at towers 0394 and 0398 were grouped together with all the 16.5 m winds and temperatures.

Table 1. List of the tower identifiers, flag as to whether the data were used in the climatology (blank = yes), the tower requirements group, and the heights (in m) of variables measured by each tower.

Sensor Complement (heights in m)					
Tower ID	Data Used?	Group	Wind	Temperature	Humidity
0001		Safety	3.6, 16.5	1.8, 16.5	N/A
0002 (0020, NW side) (0021, SE side)		Launch	3.6, 16.5, 62.2	1.8, 16.5, 62	1.8, 16.5, 62
0003		Safety	3.6, 16.5	1.8, 16.5	N/A
0006 (0061, NW side) (0062, SE side)		Launch	3.6, 16.5, 49.4, 62.2	1.8, 16.5, 62	1.8, 16.5, 62
0019		Forecast	16.5	1.8	1.8
0022		Forecast	16.5	1.8	1.8
0108		Safety	3.6, 16.5	1.8, 16.5	N/A
0110 (1101, NW side) (1102, SE side)		Launch	3.6, 16.5, 49.4, 62	1.8, 16.5, 62	1.8, 16.5, 62
0211	No	Safety	3.6, 16.5	1.8, 16.5	N/A
0300		Forecast	16.5	1.8	1.8
0303		Safety	3.6, 16.5	1.8, 16.5	N/A
0311		Safety	3.6, 16.5	1.8, 16.5	N/A
0313 (3131, SW side) (3132, NE side)		Launch	3.6, 16.5, 49.4, 62, 90, 120, 150	1.8, 16.5, 62, 150	1.8, 16.5, 62, 150
0403		Safety	3.6, 16.5	1.8, 16.5	N/A
0412		Safety	3.6, 16.5	1.8, 16.5	N/A
0415		Safety	3.6, 16.5	1.8, 16.5	N/A
0418		Forecast	16.5	1.8	1.8
0421		Forecast	16.5	1.8	1.8
0506		Safety	3.6, 16.5	1.8, 16.5	N/A
0509		Safety	3.6, 16.5	1.8, 16.5	N/A
0511	No	Launch	9.1	N/A	N/A
0512	1.8-m T only	Launch	9.1	1.8	1.8
0513	No	Launch	9.1	N/A	N/A
0714		Safety	3.6, 16.5	1.8, 16.5	N/A
0803		Safety	3.6, 16.5	1.8, 16.5	N/A
0805		Safety	3.6, 16.5	1.8, 16.5	N/A
0819		Forecast	16.5	1.8	1.8
1000		Forecast	16.5	1.8	1.8
1007		Forecast	16.5	1.8	1.8
1012		Forecast	16.5	1.8	1.8
1204		Forecast	16.5	1.8	1.8
1500	No	Forecast	16.5	1.8	1.8
1605	No	Forecast	16.5	1.8	1.8
1612		Forecast	16.5	1.8	1.8
1617	No	Forecast	16.5	1.8	1.8
2008	No	Forecast	16.5	1.8	1.8
2016	No	Forecast	16.5	1.8	1.8
2202	No	Forecast	16.5	1.8	1.8
9001		Forecast	16.5	1.8	1.8
9404		Forecast	16.5	1.8	1.8
SLC 36	No	Launch	27.4	N/A	N/A
SLC 39A (0394)		Launch	18.3	1.8, 18.3	18.3
SLC 39B (0398)		Launch	18.3	1.8, 18.3	18.3
SLC 40	No	Launch	16.5	N/A	N/A

3. METHODOLOGY

The development of a nine-year climatology involved both automated and manual QC of tower data. Once the data were quality controlled, several scripts were written to re-format data and calculate statistics on a monthly and hourly basis using the S-PLUS[®] software (Insightful Corporation 2000). Data processed in S-PLUS were then exported to Microsoft[®] Excel[®] and the General Meteorological Package (GEMPAK) software formats for post-analysis and the creation of a graphics tool. The period of record for the analysis was February 1995 to January 2004. This section describes the procedures used to generate the climatological statistics and develop the graphical means for analyzing the tower climatology results.

3.1 Data Quality Control (QC)

Five algorithms from the automated QC routine of Lambert (2002) were used to remove bad data:

- An unrealistic value check (e.g. wind speed < 0),
- A standard deviation (σ) check (e.g. temperature not within 5σ of mean),
- A peak-to-average wind speed ratio check in which the peak wind must be within a specified factor of the average wind speed (factor value dependent on average speed),
- A vertical consistency check between sensor levels at each individual tower, and
- A temporal consistency check for each individual sensor.

Only a small percentage of the data were flagged as erroneous by these QC routines: from 0.6 to 2.1% per tower and month, which resulted in a large set of good quality data for analysis. There was one known instance when good data were eliminated by the automated QC. In early May 1999, exceptionally cool temperatures occurred compared to all other months of May in the period of record. These temperatures were so unusually cool that the 5σ standard deviation check removed large portions of the data from the first couple days of the month. To alleviate this problem, the standard deviation check was modified to 10σ , but only for May data. Refer to Lambert (2002) for more specific details of the automated QC algorithm.

An initial examination of the quality-controlled data indicated that manual QC was also required for the temperature observations. The methodology for manual QC of the 1.8 and 16.5 m temperatures contains the following steps:

1. Determine the percentage availability of data at each individual tower location,
2. Generate frequency distributions of temperatures at towers with at least 70% data availability,
3. Identify the towers that have data outliers, then generate two-dimensional (2D) frequency diagrams of the temperature distributions versus UTC hour and year to determine if these outliers are bad data, and

4. Using the combined information in the 2D frequency diagrams, along with climate data, and adjacent tower information (as necessary), identify the exact times and years with bad data, and set these data to missing in the database.

This procedure was performed on a month-by-month basis in order to remove erroneous temperature observations that could not be identified by the automated routines.

3.2 Data Processing

All processing, calculations, and data stratification were conducted using the S-PLUS software. The S-PLUS software is a statistical and graphics software designed to be able to process large data sets. It has numerous features for modeling statistical processes, determining statistical distributions, displaying graphical data, and running batch scripts. One of the most helpful features of S-PLUS used for this climatology is its ability to calculate statistics based on categorical data stratification. For example, the mean temperature could be computed for each category of hour (ranging from 00 to 23 UTC) or pre-defined wind direction bin. The variables and heights processed for climatology consisted of temperature at 1.8 m and 16.5 m, temperature at 16.5 m minus temperature at 1.8 m (representing near-surface stability), wind speed at 16.5 m, and wind direction standard deviation at 16.5 m. Dew point temperature or relative humidity data were not examined for this climatology.

The following statistics were computed for each of the variables and heights noted above:

- Mean,
- Standard Deviation,
- Bias,
- Percent data availability, and
- Data count and climatological probability for wind direction bins.

All of the above quantities were calculated on an hourly basis for all years collectively in each individual month, so as to develop a monthly climatology of the diurnal variations of each variable/height. Data were also stratified by wind direction bins, every 45° from 0° to 360° .

The climatological probabilities of wind direction bins were computed by simply dividing the number of observations in a particular wind direction bin by the total count of observations for all wind directions. These probabilities were calculated for each tower individually as well as all towers used in the combined climatology.

Those towers labeled as not used in column 2 of Table 1 had insufficient data availability year-round, and were therefore excluded from all portions of the climatology. Among the towers used in the climatology (see columns 1 and 2 in Table 1), only towers with at least 70% overall data availability in a given month were included in the climatology for that month. The wind direction stratification statistics were conducted using all towers except those listed as not used in column 2 of Table 1.

3.3 Analysis and Display Tools

After all statistics were processed using S-PLUS, the resulting data were exported into Excel and GEMPAK files for analysis and display. The S-PLUS statistics were formatted for Excel pivot charts and tables, which served as the primary mechanism for displaying the tower climatology results graphically. The GEMPAK software was used to develop geographical plots and contours of the climatological statistics so that the geographical variability across the KSC/CCAFS tower network could be examined.

4. SELECTED RESULTS

The climate of east-central Florida is largely driven by the complex land-water interfaces of the Atlantic Ocean and rivers/lagoons interacting with the land areas of KSC, CCAFS, and the Florida mainland (Figure 2). Towers with close proximity to water typically have much warmer nocturnal temperatures and substantially higher wind speeds throughout the year. The following sub-sections highlight the major mesoscale variations in the climatology of KSC/CCAFS.

4.1 Climatological Probabilities of Wind Directions

The diurnal distribution of climatological probabilities of wind direction ranges (defined in Table 2) during the month of July for the entire tower network is shown in Figure 5. The hourly values ranging from 00 to 23 UTC reveal the mean diurnal variation in the climatological probabilities of wind direction that typify the Florida warm season. From the mid-morning to early afternoon hours (~1500–1800 UTC), the east and southeast probabilities increase rapidly, representing the typical onset time of the sea breeze. After 1800 UTC, the wind directions steadily rotate clockwise, with the south-southeast bin (180°) probabilities peaking at 0000 UTC, the south-southwest bin (225°) reaching a maximum at 0600 UTC, and the west-southwest bin (270°) peaking at 1200 UTC. This steady clockwise rotation in the prevailing wind direction illustrates the impact of the Coriolis force on the local wind field across east-central Florida. The land-sea thermal contrast causes the initial rapid increase in onshore (easterly) winds during the midday hours, but then the Coriolis acts to rotate the winds in a clockwise sense by an average of 45° every six hours.

A distinct annual trend in the favored wind directions is evident from the diurnal probabilities plots extended to all months, as shown in Figure 6. North and northwest winds (315° and 360° bins) are most prevalent from November to February (~20–30%), then steadily decrease in probability, reaching a minimum in June and July (~5–10%). Thereafter, the probabilities of north and northwest winds increase again, particularly in October. Conversely, the southeast and south wind direction bins (135° and 180°) experience a minimum in probability from November to February (~5–15%),

steadily increase to a maximum in July (~30–40%), and then decrease thereafter, especially from September to October. Most of the other wind direction bins fluctuate between 5–15% probabilities throughout the year, except for the southwest and west bins during the summer months. A much higher occurrence of southwest and west winds is found during the nocturnal and early morning hours from June to August. Also note the relatively high occurrence of easterly winds during October, attributed to the first cool fronts of the autumn season, and the prevalence of high pressure systems to the north of Florida.

Table 2. Wind direction bin labeling convention.

Wind Direction Bin Label	Valid Wind Direction Range
45°	0° < wind direction ≤ 45°
90°	45° < wind direction ≤ 90°
135°	90° < wind direction ≤ 135°
180°	135° < wind direction ≤ 180°
225°	180° < wind direction ≤ 225°
270°	225° < wind direction ≤ 270°
315°	270° < wind direction ≤ 315°
360°	315° < wind direction ≤ 360°

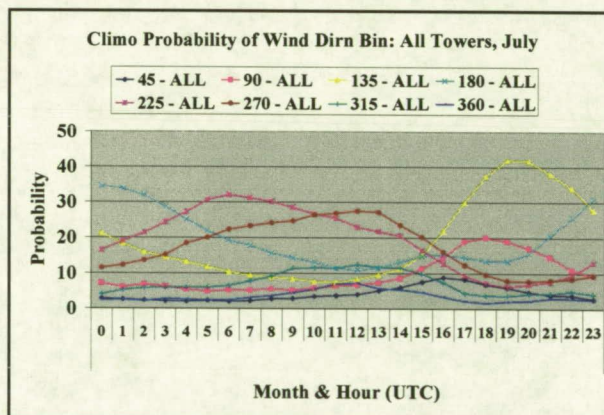


Figure 5. The climatological probability of the wind direction falling into eight different bins for all towers combined during the nine-year period of record, valid for July only. Twenty-four hourly climatological probabilities are given along the x-axis.

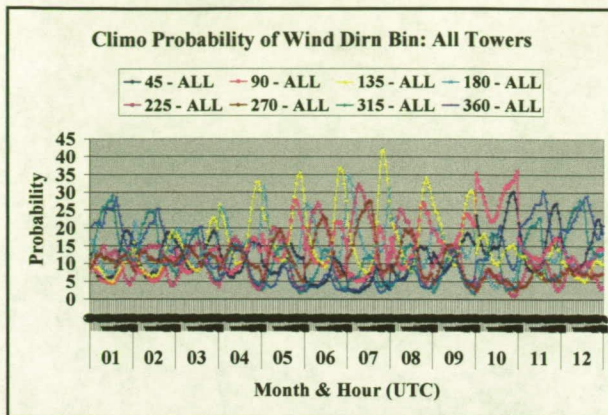


Figure 6. The climatological probability of the winds falling into eight different direction bins for all towers combined during the nine-year period of record. Twenty-four hourly climatological probabilities are given in each month along the x-axis.

4.2 Temperature/Low-Level Stability

Up to a 5 C difference occurred in the mean 1.8 m temperature across the network throughout the year, most notable in the pre-dawn hours. Even larger 1.8 m temperature variations were found within specific wind direction ranges. The variations in 16.5 m temperatures were much smaller across KSC/CCAFS, so the near-surface stability (16.5 m minus 1.8 m temperature) was primarily a function of the 1.8 m temperatures.

Figure 7 shows that the coastal and causeway towers had considerably higher mean temperatures than the overall network during the nocturnal hours for all months of the year. Meanwhile, tower 0819 usually had the highest mean 1.8 m temperatures during the time of maximum heating and the lowest mean temperatures at night.

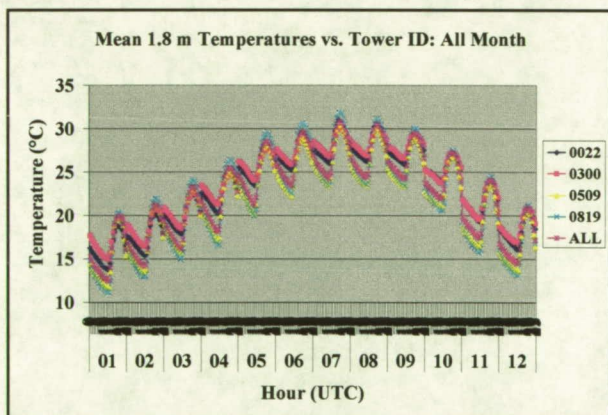


Figure 7. The diurnal range in mean 1.8 m temperatures during all months of the year for coastal tower 0022, causeway tower 0300, Merritt Island tower 0509, and mainland tower 0819, and all towers averaged together (ALL). The x-axis contains 24 hours embedded within each month.

The mean temperatures across the tower network had much more variability with wind direction during the cool-season months than during the warm season. From November to February, the mean temperatures for the northwest and north bins (315° and 360° in Figure 8a, or 271°–360° wind directions) were 5–10 C or more cooler than the southeast and south bins (135° and 180°), which tended to be the warmest during these months. The 271°–315° wind directions were the coolest of all, with a minimum mean temperature of 8 C in January. Any wind direction with a southerly component had the highest mean temperatures, with the southeasterly winds having the highest mean nocturnal temperatures in most cool-season months.

Unlike the cool season, the warm season months exhibited much less variation in the mean 1.8 m temperatures as a function of wind direction. The mean temperatures for most wind direction bins were within 2.5 C of one another, particularly from July to September (Figure 8b). May had the largest range of mean temperatures versus wind direction during the day, and October had the largest range at night; however, October tends to be a transition month between the warm/wet and cool/dry season.

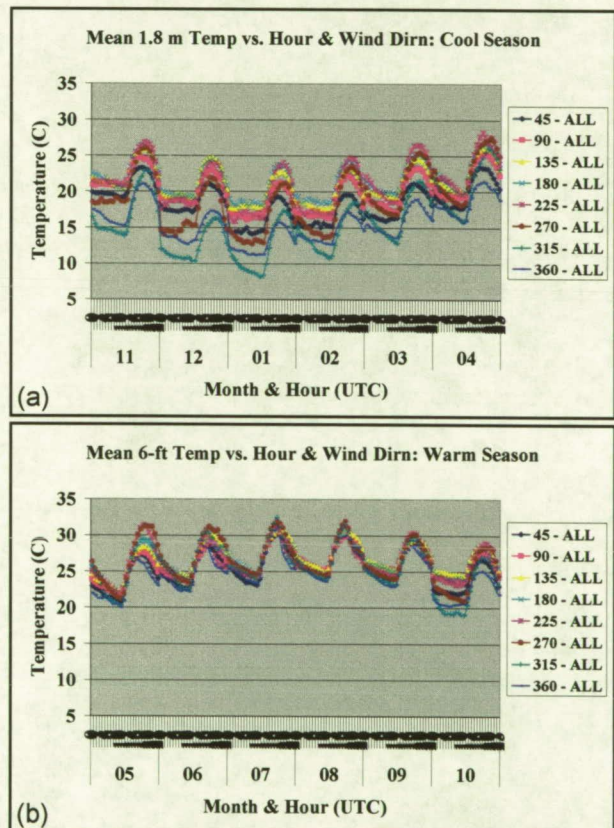


Figure 8. The hourly mean 1.8 m temperatures versus wind direction bin, averaged over all towers in the KSC/CCAFS network, valid for (a) the cool-season months (November–April), and (b) the warm-season months (May–October).

The difference between the 16.5 and 1.8 m temperatures (i.e. near-surface stability) shows some interesting variation throughout the year. From March to September, the mean near-surface stability tends to increase steadily during the night until sunrise, thereafter decreasing abruptly with the onset of solar heating (Figure 9). From November to January, a different pattern appears in the nocturnal mean near-surface stability. The stability values peak at about 0300 UTC and then gradually decrease during the remainder of the night. The shift in the nocturnal stability pattern occurs at nearly all towers within the network. October and February appear to be transition months between these distinctly different behaviors. This climatological behavior in near-surface stability could be used as first-order guidance by the 45th Space Wing Range Safety. These data could help Range Safety assess the times of the day and year when stability poses the greatest risk for a potentially hazardous plume or shock wave adversely affecting populated areas during launch operations at CCAFS.

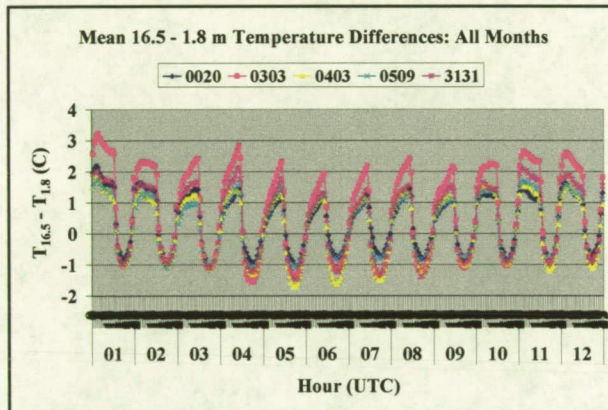


Figure 9. The diurnal range in the mean 16.5 m minus 1.8 m temperatures for all months of the year at the selected towers shown in the legend.

The physical explanation for the different near-surface stability behaviors between the winter months and rest of the year can be found in the mean wind speed plot at tower 0303 (Figure 10). During the months when stability increased steadily throughout the night, the mean wind speeds at tower 0303 tended to decrease steadily during the same hours. However, during the winter months, wind speeds initially dropped rapidly with sunset, but then leveled off for the remainder of the night instead of continuing to decrease. Similar nocturnal mean wind speed trends occurred at most other towers in the network (not shown). Therefore, the stability peak near 0300 UTC during the winter months is probably mechanical in nature, since the initial sharp decrease in wind speeds at sunset led to a rapid decrease in 1.8 m temperatures. The mean stability then levels off or slightly decreases during the remainder of the night because of the nearly constant wind speed that prevailed due to a higher frequency of synoptic-scale weather features in the Florida cool season.

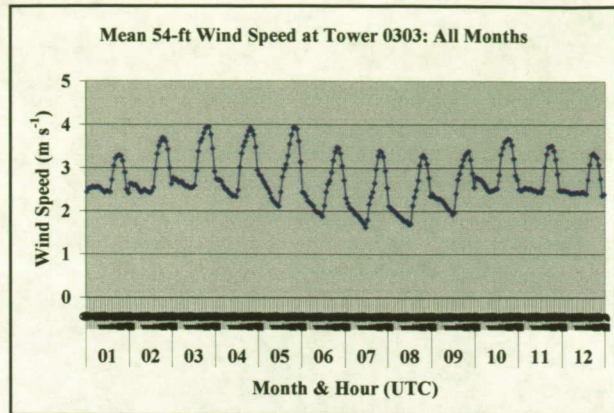


Figure 10. Hourly mean wind speeds at tower 0303 for all months of the year.

4.3 Wind Speed

Mean domain-wide wind speeds were generally $2\text{--}3\text{ m s}^{-1}$ during the nocturnal hours and $3.5\text{--}4.5\text{ m s}^{-1}$ during the day. The strongest mean nocturnal wind speeds of $3\text{--}3.5\text{ m s}^{-1}$ occurred from October to March (the synoptic season). Meanwhile, the strongest mean daytime wind speeds of $4\text{--}5\text{ m s}^{-1}$ occurred from February to May, probably due to a combination of synoptic systems and strengthening sea-breeze circulations during this latter portion of the Florida dry season.

Coastal and causeway towers tended to have mean wind speeds $1\text{--}2\text{ m s}^{-1}$ stronger than the overall network mean. Meanwhile, mainland towers had mean speeds weaker than the network mean by about the same magnitude. The resulting gradient in the mean wind speed across the network was typically $2.5\text{--}4\text{ m s}^{-1}$ over a distance of $20\text{--}30\text{ km}$, with the strongest speeds occurring along the Atlantic coastal towers.

Figure 11 illustrates this contrast between the winds speeds at Atlantic coastal and mainland towers. The coastal tower 0022 and causeway tower 0300 generally had much higher wind speeds compared to Merritt Island tower 0509 and mainland tower 0819. Tower 0022 and 0300 were both much higher than the overall network averages (ALL in Figure 11), and had very similar diurnal speed distributions except for October through January. During these months, nocturnal wind speeds were much higher at coastal tower 0022 compared to the causeway tower, particularly in October, when east and northeasterly winds tended to occur more frequently than other directions (Figure 6). The predominance of northeasterly wind directions led to stronger winds along the immediate coast compared to the causeway tower, because of the frictional effects as winds cross CCAFS upstream of tower 0300.

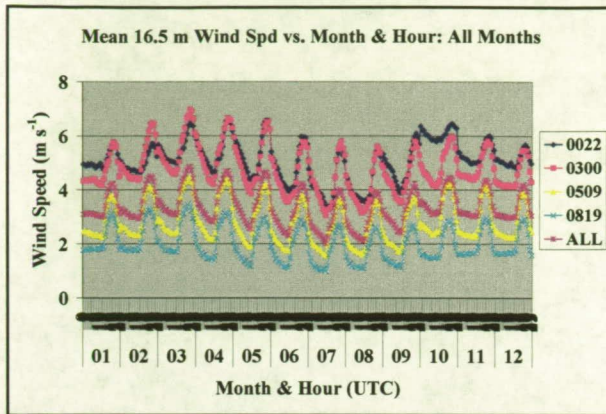


Figure 11. Hourly mean wind speeds for all months of the year at towers 0022, 0300, 0509, 0819, and all towers averaged together (ALL).

In the spring and summer months when daily sea breezes predominate, the time of maximum wind speeds was delayed by a few hours after peak heating. Meanwhile, during the winter months, the time of the maximum mean wind speed corresponded well with the time of maximum heating. These relationships are illustrated in Figure 12, which shows an overlay of the hourly mean temperature differences between the near-shore buoy 41009 and the overall tower network average of 1.8 m temperature ($T_b - T_n$), and the mean wind speed normalized by the monthly mean value (all-mean). This normalization is done by simply subtracting each month's overall mean speed from the individual hourly mean wind speeds, in order to have similar scales along the y-axis for easier comparison. Since the mean air temperature at the buoy varies only by about a degree Celsius on a diurnal basis, most of the variation in $T_b - T_n$ results from the diurnal heating cycle in the tower network. Minimum $T_b - T_n$ corresponds to the time of maximum heating within the tower network.

During the spring and summer months, a 3–4 hour separation occurs between the time of maximum heating (given by solid lines in Figure 12a) and the time of maximum mean wind speed (given by dashed lines). The delay in peak wind speeds during the spring and summer is consistent with the high frequency of sea breezes, caused by the temperature contrasts between the air over land and water. The sea breeze circulation strength actually peaks after the time of maximum contrast between the air temperatures over land and water. Convective outflows may also play a minor role in the higher magnitude of the mean wind speeds during the late afternoon hours in the summer months.

Meanwhile, from November to January, when sea breezes occur less frequently, the time of maximum heating and peak wind speed are nearly coincident (Figure 12b). Also, the wind speed and land-ocean temperature differential curves are 180° out of phase, indicating that wind speeds increase in proportion to the daytime heating across the tower network. These relationships suggest that synoptic pressure gradients and vertical mixing through surface heating and destabilization drive the strength of winds during the winter months.

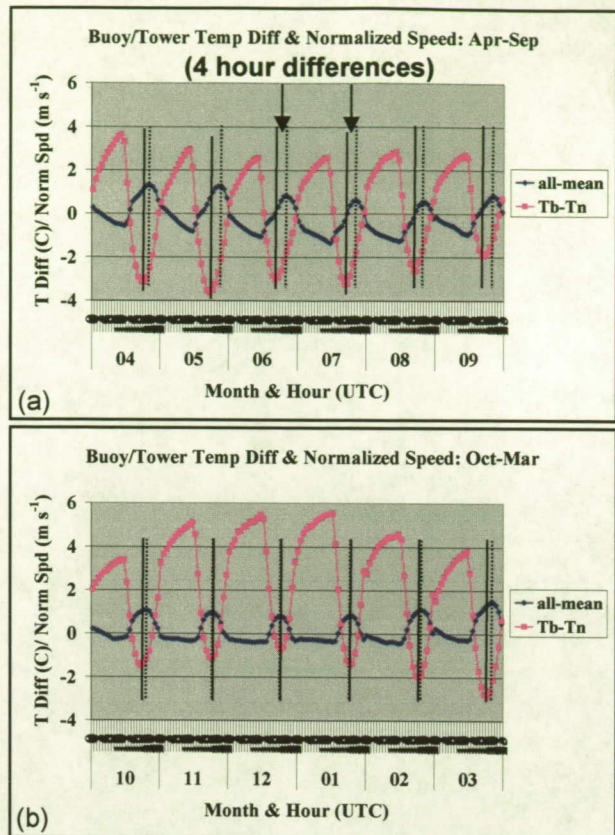


Figure 12. Plot of the hourly differences between the buoy and tower network mean 1.8 m temperatures ($T_b - T_n$), and the hourly mean wind speed normalized by the monthly mean wind speed (all-mean), valid for the months of (a) April to September, and (b) October to March. Solid vertical lines represent the time of minimum $T_b - T_n$ (i.e. time of maximum tower temperatures) and dashed vertical lines represent the time of the maximum mean wind speed.

The bias of wind speed under specific wind directions is nearly invariant with the season or time of year, based on the plots of selected towers in Figure 13. During both the cool season (Figure 13a) and warm season (Figure 13b), coastal tower 0022 had the highest positive bias with northeast to east winds, and also for westerly to northwesterly winds. The causeway tower 0300 exhibited the largest positive wind speed bias for south-southeast winds (180° bin) during both seasons, as these directions create the largest fetch over water upstream of this tower (refer to Figure 2).

Conversely at mainland tower 0819, a negative bias between -1 and -2 m s^{-1} prevailed year-round for all wind directions except for the west/northwest direction (315° bin), which yielded less negative biases. The CCAFS tower 0303 and Merritt Island towers 0509 and 3131 fell between the coastal/causeway and mainland biases. Since the wind speed variations by wind direction across KSC/CAFS are independent of the time of year, it appears that the geographical features of KSC/CAFS are the primary drivers for the observed patterns of wind speed variations.

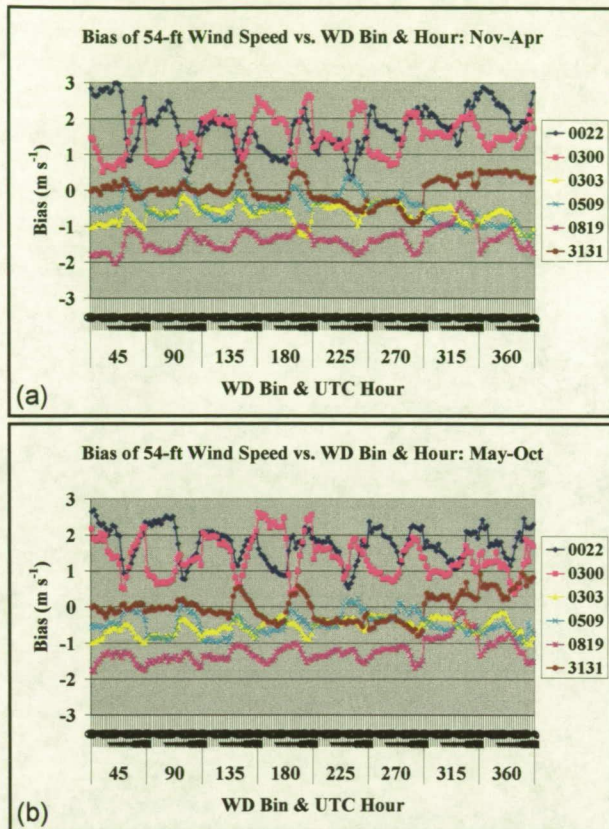


Figure 13. The hourly bias of 16.5 m wind speeds (m s^{-1}) as a function of wind direction bin at coastal tower 0022, causeway tower 0300, CCAFS tower 0303, Merritt Island tower 3131 (i.e. 0313), and mainland tower 0819, valid for (a) the cool-season months, and (b) the warm season months.

5. SUMMARY

This paper presented an excerpt from a nine-year, monthly meso-climatology of temperatures and winds at 1.8 m and 16.5 m for the KSC/CCAFS tower network in east-central Florida. Data were analyzed at 33 selected tower locations. All 33 towers provided 1.8 m temperature and 16.5 m wind data archived at 5 minute intervals, while 19 towers also provided archived 16.5 m temperature data every 5 minutes.

The meso-climate of KSC/CCAFS is largely driven by the complex land-water interfaces of KSC/CCAFS. Towers with close proximity to water typically exhibited much warmer nocturnal temperatures and substantially higher wind speeds throughout the year. Up to a 5 C difference occurred in the mean 1.8 m temperature across the tower network throughout the year, most notable in the pre-dawn hours.

Mean domain-wide wind speeds were generally $2\text{--}3 \text{ m s}^{-1}$ during the nocturnal hours and $3.5\text{--}4.5 \text{ m s}^{-1}$ during the day. The strongest mean nocturnal wind speeds occurred from October to March (the synoptic season). The strongest mean daytime wind speeds occurred from February to May, probably due to a

combination of synoptic systems and strengthening sea-breeze circulations.

Coastal and causeway towers tended to have the strongest overall mean wind speeds while the mainland towers had the weakest speeds. The resulting gradient in the mean wind speed across the network was typically $2.5\text{--}4 \text{ m s}^{-1}$ over a distance of 20–30 km, with the strongest speeds occurring at the Atlantic coast.

Most biases were largely a result of the geographical variability, which tended to mask any smaller instrument, processing, and exposure errors. The coastal and causeway towers had cool (warm) biases during the day (night) compared to Merritt Island and mainland towers. The towers located near water bodies also had high wind speed biases, whereas the mainland towers experienced low wind speed biases relative to the overall network average. Since all the space launch complexes are nearly coincident with the Atlantic coast, forecasters can expect vehicles wind exposures on the high end of the climatology results.

6. REFERENCES

- Computer Sciences Raytheon (CSR), 2000: *45th Space Wing Eastern Range Instrumentation Handbook*, Computer Sciences Raytheon Inc., 758 pp.
- Harms, D. E., B. F. Boyd, M. S. Gremillion, M. E. Fitzpatrick, and T. D. Hollis, 2001: Weather support to space launch: A quarter-century look at weather instrumentation improvements. Preprints, *11th Symp. on Meteorological Observations and Instrumentation*, Albuquerque, NM, Amer. Meteor. Soc., 259–264.
- Haugen, D. A., and J. J. Fuquay, 1963: The ocean breeze and dry gulch diffusion programs Volume I. U. S. Air Force Project Order No. 61-577, Air Force Cambridge Research Laboratories, Hanscom Field, MA, 252 pp.
- Haugen, D. A., and J. H. Taylor, 1963: The ocean breeze and dry gulch diffusion programs Volume II. U. S. Air Force Project Order No. 61-577, Air Force Cambridge Research Laboratories, Hanscom Field, MA, 112 pp.
- Insightful Corporation, 2000: *S-PLUS® 6 User's Guide*, Insightful Corp., Seattle, WA, 470 pp.
- Lambert, W. C., 2002: Statistical short-range guidance for peak wind speed forecasts on Kennedy Space Center/Cape Canaveral Air Force Station: Phase I results. NASA Contractor Report CR-2002-211180, Kennedy Space Center, FL, 39 pp. [Available from ENSCO, Inc., 1980 N. Atlantic Ave., Suite 230, Cocoa Beach, FL 32931.]
- Watson, A. I., R. E. Lopez, R. L. Holle, J. R. Daugherty, and R. Ortiz, 1989: Short-term forecasting of thunderstorms at Kennedy Space Center, based on the surface wind field. Preprints, *Third Conference on Aviation Systems*, Anaheim, CA, Amer. Meteor. Soc., 222–227.